Optical Trapping and Fundamental Studies of Atomic Fermi Gases

J. E. Thomas, J. Joseph, B. Clancy, L. Luo,
J. Kinast and A. Turlapov

Department of Physics, Duke University, Durham, N.C. 27708-0305, USA

ABSTRACT

Optical traps provide tight confinement and very long storage times for atomic gases. Using a single focused beam from a CO_2 laser, we confine a mixture of spin-up and spin-down fermionic ^{6}Li atoms, achieving storage times of ten minutes, and evaporative cooling to quantum degeneracy in seconds. A bias magnetic field tunes the gas to a collisional (Feshbach) resonance, producing extremely strong spin-pairing. This system now tests current many-body predictions for high-temperature superconductors, universal interactions in neutron stars, and hydrodynamic flow of quark-gluon plasmas, a state of matter that existed microseconds after the Big Bang.

Keywords: Optical traps, Fermi gases, All-optical cooling

1. INTRODUCTION

Optical traps are nearly ideal containers for confining ultracold atomic and molecular gases. Direct evaporative cooling of atomic and molecular gases in optical traps also simplifies production of these cold quantum gases. All-optical techniques are now being used to create and study Bose-Einstein condensates (BEC's) of atoms[1,2] and molecules,[3] weakly interacting Fermi gases[4] and strongly-interacting Fermi gases.[5,6] The simplest optical trap is a focused laser beam, tuned well below the nearest optical resonance. In that case, atoms or molecules are attracted to the focus. When the trap is tuned far below resonance,[7] the confining potential is nearly state independent, and proportional to the trapping laser intensity.

Nearly ideal, conservative optical traps are constructed by reducing residual heating sources. Heating arises from Larmor scattering of the trapping laser light,[8] from intensity and position noise in the trapping laser beams,[9,10] and from small-angle background gas collisions.[11,12]

CO_2 lasers, with a 10.6 μm wavelength, are particularly well suited for optical traps. CO_2 lasers produce very high power $\simeq$ 100 W or more, and correspondingly deep traps. The heating rate due to Larmor scattering is reduced to a minimum, since the scattering rate[8] scales $1/\lambda^3$ and the heating rate as $1/\lambda^5$. For our CO_2 laser trap, the intensity at the focus is 2 MW/cm^2, yet the optical scattering rate is only 2 photons/hour with a corresponding heating rate of only 18 pK/s!

CO_2 lasers, especially those from the laser radar industry, are especially quiet. Intensity noise can cause exponential heating,[9,10] but for our current trap, the estimated time constant, based on the measured laser intensity noise power spectrum, is found to be 7 hours! By using a very high vacuum, $< 10^{-11}$ Torr, heating arising from background gas collisions is reduced to negligible levels. Then the time that an atom or molecule can remain in the trap is determined by the time required for a background gas atom to scatter an atom out of the trap, which is about 400 seconds at $< 10^{-11}$ Torr.

Since atoms are stored in a nearly conservative potential, stable optical traps are very well suited to producing ultracold quantum gases by evaporative cooling. Optical traps can be directly loaded from a standard magneto-optical trap (MOT) which serves as a cold atom source. Collisions between atoms in the optical trap result in evaporative cooling. By lowering the intensity of the trapping laser beam, efficient evaporative cooling is achieved, with relatively small reduction in the number of atoms.[13] All-optical production of a quantum gas by

Further author information: (Send correspondence to J. E. T.)
J. E. T.: E-mail: jet@phy.duke.edu, Telephone: 1 919 660 2508

Optical Trapping and Optical Micromanipulation III, edited by Kishan Dholakia, Gabriel C. Spalding,
Proc. of SPIE Vol. 6326, 632602, (2006) · 0277-786X/06/$15 · doi: 10.1117/12.678574

this method was first demonstrated for a BEC of ^{87} Rb, and shortly thereafter, for a degenerate Fermi gas of ^{6}Li.[4]

As noted earlier, for large detuning of the trapping laser beam from the atomic resonance, the confining potential is independent of applied magnetic fields. Hence, optical traps are well suited for applications requiring strong magnetic fields, as needed for the study of Feshbach resonances.[5,14]

Optical traps provide a state-independent confining potential which is essential for the study of interacting ultracold Fermi gases: In Fermi gases at low temperature, where s-wave scattering dominates, the Pauli exclusion principle suppresses collisions in a single component gas. Hence, more than one spin state must be simultaneously trapped.

Currently, experiments with optically-trapped, strongly-interacting Fermi gases[5,15] provide tests of nonperturbative many-body theories in a variety of fields, from neutron stars and nuclear matter[16–18] to quark-gluon plasmas[19] and high temperature superconductors.[20] In contrast to other Fermi systems, interactions in the ultra cold atomic gases are tunable at will using the Feshbach resonance phenomenon .[5,21,22] Near the resonance, the s-wave scattering length and the cross section of cold s-wave collisions between spin-up and spin-down atoms changes smoothly from 0 to large values (providing strong interactions) in response to an external magnetic field.

The strongly-interacting regime of an interacting Fermi gas is also referred to as the BEC-to-BCS crossover regime. In this regime, evidence of new, high-temperature superfluidity has been found in the studies of collective dynamics.[5,23–25] Microscopic properties of the superfluid have been probed by detecting pairs of Fermi atoms in projection,[26,27] in rf spectroscopy experiments,[28,29] and in optical spectroscopy measurements of the order parameter.[30] Recent measurements of the heat capacity[31] and collective damping[32] near resonance reveal transitions close to the temperature predicted for the onset of Fermi superfluidity. Superfluidity is confirmed by the observation of quantized vortex lattices.[33]

Theoretical predictions spanning nearly thirty years and several disciplines have been made for the many-body ground state of a strongly-interacting two-component Fermi system, characterized by two-body scattering via a short range potential with a very large scattering length.[16,17,34,35] Far from resonance, the system is weakly interacting and well understood, establishing a reference for experiments and theories: At magnetic fields well above the resonance, weakly attractive atoms form Cooper pairs in agreement with the Bardeen–Cooper–Schrieffer (BCS) theory of superconductivity/superfluidity; and below the resonance, spin-up and spin-down atoms are joined into dimer molecules, which form a Bose–Einstein condensate (BEC).[3,36–38]

Near a broad Feshbach resonance, Fermi gases also exhibit universal interactions[5,16,39] and universal thermodynamics,[40] i. e., the properties of the gas are independent of microscopic details of interaction and are the identical to those of other resonantly-interacting Fermi systems. In that case, the interaction energy is a universal fraction, denoted β, of the local kinetic energy.[5,39] The universal interaction energy was originally explored theoretically in the context of nuclear matter,[16,17] and has been the subject of new calculations[18,41–44] and recent measurements by several groups based on the release energy,[5] cloud size[31,39,45,46] and momentum distribution.[47,48] Currently, there is still controversy regarding the correct value of β. On-resonance speed of sound measurements provide a new method for measurement of this universal quantity.

The zero-temperature equation of state has been quantitatively tested by two different methods – expansion of the gas[5,38,39] and oscillations of a trapped cloud.[23–25] These measurements probe the dependence of the pressure on the density, but they are not sensitive to the absolute pressure. In contrast, sound propagation[49–51] provides a new direct probe of the equation of state, a central result of predictions.[52] Moreover, sound propagation is sensitive to the absolute pressure, which makes it ideal for distinguishing which theories have the correct ground state.

2. EXPERIMENTAL SYSTEM

We prepare a highly degenerate, strongly-interacting Fermi gas of ^{6}Li. This is accomplished using evaporation of an optically-trapped, 50-50 mixture of spin-up/down states at 840 G, just above the center of a broad Feshbach resonance.[5,23,25,31,32] To reduce the temperature, we do not employ a magnetic sweep from a BEC of molecules, in contrast to several other groups.[24,27,28,33,38,45] Instead, we evaporate directly in the strongly attractive,

unitary regime: We simply exploit the large collision cross section and the rapid vanishing of the heat capacity with decreasing temperature, which is especially effective in the superfluid regime. These properties make the gas easier to cool.

In the forced evaporation, the depth of CO_2 laser optical trap is reduced to 1/580 of its maximum value, and then recompressed to 4.6% of the maximum trap depth for most of the experiments. From the trap frequencies measured under these conditions and corrected for anharmonicity, we obtain: $\omega_\perp = \sqrt{\omega_x \omega_y} = 2\pi \times 1696(10)$ Hz, $\omega_x/\omega_y = 1.107(0.004)$, and $\lambda = \omega_z/\omega_\perp = 0.045$. Then, $\bar{\omega} = (\omega_x \omega_y \omega_z)^{1/3} = 2\pi \times 589(5)$ Hz is the mean oscillation frequency. For most of the data reported, the total number of atoms is $N = 2.0(0.2) \times 10^5$. The corresponding Fermi temperature at the trap center for a noninteracting gas is $T_F = (3N)^{1/3}\hbar\bar{\omega}/k_B \simeq 2.4\,\mu$K, small compared to the final trap depth of $U_0/k_B = 35\,\mu$K (at 4.6% of the maximum trap depth). The coupling parameter of the strongly-interacting gas at $B = 840$ G is $k_F a \simeq -30.0$, where $\hbar k_F = \sqrt{2m\,k_B T_F}$ is the Fermi momentum, and $a = a(B)$ is the zero-energy scattering length estimated from the measurements of Bartenstein et al.[53]

3. UNIVERSAL THERMODYNAMICS

As noted above, near a broad Feshbach resonance, a strongly-interacting gas obeys the universal hypothesis, where the interparticle spacing, $1/k_F \propto n^{-1/3}$, and hence the density n, determines the natural length scale. In this regime, where $k_F a >> 1$, the local thermodynamic properties are then functions only of the density and temperature, the same variables that describe a noninteracting Fermi gas. The universal hypothesis has directly measurable consequences, some of which we will describe briefly.

3.1. Virial Theorem

According to the universal hypothesis, the local pressure P must be a function of the local density and temperature.[40] In this case, a strongly-interacting Fermi gas must obey the virial theorem for a noninteracting gas at all temperatures, as we now show. One can readily show by elementary thermodynamic arguments that if $P = P(n, T)$, then

$$P = \frac{2}{3}\,\varepsilon(\mathbf{x}), \tag{1}$$

where $\varepsilon(\mathbf{x})$ is the local energy density, i.e., the sum of the local kinetic and interaction energies.[40,54]

Balance of the pressure and trapping forces in a harmonic potential requires that $N\langle U\rangle = (3/2)\int d^3\mathbf{x}\, P(\mathbf{x})$, where $\langle U\rangle$ is the average potential energy per particle. Using $\int d^3\mathbf{x}\,\varepsilon(\mathbf{x}) = E - N\langle U\rangle$, one obtains[54]

$$N\langle U\rangle = \frac{E}{2}. \tag{2}$$

This result is remarkable: Analogous to an ideal noninteracting gas, a trapped, strongly-interacting, unitary gas, comprising condensed superfluid pairs, noncondensed pairs, and unpaired atoms, should obey the virial theorem. Since $\langle U\rangle \propto \langle x^2\rangle$, the mean square transverse radius $\langle x^2\rangle$ of the trapped cloud should scale linearly with the total energy, as verified in our experiments, see § 4.2. Using Eq. 2, we see that the energy of a harmonically trapped ideal gas or a unitary gas can be determined from the mean square cloud size

$$E/N = 3m\omega_x^2\langle x^2\rangle. \tag{3}$$

3.2. Spatial Distribution and Measurement of the Interaction Energy

At zero temperature, the local energy per particle for a unitary gas is just $(3/5)(1+\beta)\,\epsilon_F(n)$ where $\epsilon_F(n) = \hbar^2(3\pi^2 n)^{2/3}/(2m)$ is the local Fermi energy of a noninteracting Fermi gas and β is a measurable universal constant[5,16,39] which denotes the ratio of the local interaction energy to the local kinetic energy at zero temperature. For an ideal gas, $\beta_{ideal} = 0$, while for a unitary gas, $\beta < 0$, denoting an effectively attractive interaction.

For a zero temperature unitary gas, the net effect of the interactions is then equivalent to changing the bare mass m to an effective mass,[17,31] $m^* = m/(1+\beta)$. The Fermi temperature for a harmonically trapped, noninteracting gas, is given by $T_F = (3N)^{1/3}\hbar\bar{\omega}/k_B$. Since the effective mass for the strongly-interacting gas

is given by $m^* = m/(1+\beta)$, the effective oscillation frequency is altered by a factor of $\sqrt{1+\beta}$, and the Fermi temperature for the strongly-interacting gas is given by

$$T_F' = T_F\,\sqrt{1+\beta}. \tag{4}$$

The equation of state at $T = 0$ yields precisely a zero temperature, Thomas-Fermi profile, $n_0(\mathbf{x})$, for which the Fermi radius is $\sigma_x' = \sqrt{2k_B T_F'/m\omega_x^2} = (1+\beta)^{1/4}\sigma_x$,[39] where σ_x is the Fermi radius for a noninteracting gas. The $y-z$ integrated one-dimensional profile takes the form,

$$n(\sigma_x, T=0) = \frac{16\,N}{5\pi\sigma_x'}\left(1-\frac{x^2}{\sigma_x'^2}\right)^{5/2} \tag{5}$$

We find that the measured spatial profiles of our coldest clouds assume nearly the shape of a zero-temperature Thomas-Fermi profile.[5,39,55] Measurements of the cloud radii can then be used to determine β.[31,39,45]

We obtain β by comparing the transverse radius of the trapped cloud for the interacting gas with that of the noninteracting gas.[39] For the noninteracting gas, we use either the calculated σ_x or the radius measured after ballistic expansion scaled to the in-trap dimension. For the interacting gas, we obtain σ_x' after hydrodynamic expansion for 1 ms. We find that at 840 G, $\beta[840] = -0.49(0.04)$ (statistical error only). Similar results are obtained by measurements on the axial dimension of the trapped cloud without expansion[45] and by direct measurements of the interaction energy.[47] There is some discrepancy between the measurements that may arise from the sensitivity of β to the precise location of the Feshbach resonance,[45] which in ^{6}Li has been most recently measured by radiofrequency methods.[53]

Using the results of a recent mean field model of the BEC-BCS crossover regime,[56] we can use our measurements at 840 G to estimate the value of β at resonance, where $B = 834$ G, and $1/(k_F a) = 0$. Near resonance, one obtains[56]

$$\beta[1/(k_F a)] = \beta - \frac{0.64}{k_F a}. \tag{6}$$

For our trap conditions, $k_F a = -30$ @ 840 G and $\beta[1/(k_F a)] = -0.49$ from our measurements. Hence, we find $\beta = -0.51(0.04)$. This is in good agreement with recent measurements based on the axial cloud size,[46] where $\beta = -0.54(0.02)$. These results are in good agreement with recent calculations, $\beta = -0.56$,[18] $\beta = -0.545$,[41] and with the simple mean field model, $\beta = -0.564$.[56]

3.3. Universal Hydrodynamics and Evidence for Superfluidity

At zero temperature, the local pressure of the trapped gas differs from the Fermi pressure of a noninteracting gas by a factor of $1+\beta$ and the pressure then scales as $n^{5/3}$. In this case, upon release from a harmonic trap, the expansion dynamics are governed precisely by a scale transformation, where the density evolves according to $n(\mathbf{x},t) = n_0(\tilde{\mathbf{x}})/\Gamma$, where $\tilde{x} = x/b_x(t)$, $\Gamma = b_x b_y b_z$, and $b_i(t)$ is a hydrodynamic expansion factor.[5,57] The predicted hydrodynamic expansion for release from a cigar-shaped trap is highly anisotropic, and independent of β, i.e., the gas expands rapidly in the originally narrow direction while remaining nearly stationary in the long direction as observed in experiments.[5]

The breathing mode frequencies take on universal values when the local pressure scales as $n^{5/3}$, and are independent of β. For a cylindrically-symmetric trap, the radial breathing mode frequency for a zero temperature hydrodynamic gas is given by

$$\omega_{hydro} = \sqrt{\frac{10}{3}}\,\omega_\perp = 1.83\,\omega_\perp. \tag{7}$$

For the conditions of our trap, which deviate slightly from cylindrical symmetry, exact diagonalization of the linearized hydrodynamic equations yields $\omega_{hydro} = 1.84\,\omega_\perp$. One can generalize these arguments to show that they hold at all temperatures where the gas expands hydrodynamically *under isentropic conditions.*[54]

We excite the radial breathing mode by releasing the gas for 25μs, and recapturing the cloud. The width is measured as a function of hold time prior to release and imaging. Fig. 1 shows the data at the lowest temperature. By fitting a damped sinusoid to the data, we find that $\omega/\omega_\perp = 1.832(0.012)$,[23,25,32] in very good agreement with

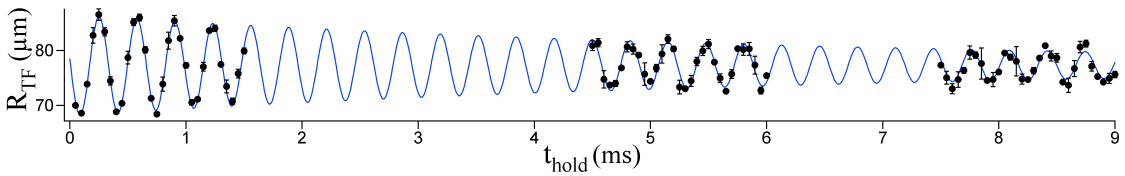

Figure 1. Radial breathing mode amplitude versus hold time.

the predicted value, 1.84.

These collective mode measurements also provide strong evidence for superfluid hydrodynamics in a strongly-interacting Fermi gas. We find that the damping rate of the breathing mode decreases as the temperature is decreased, although the frequency is hydrodynamic. This behavior is inconsistent with collisional hydrodynamics, since the collision rate γ is expected to be suppressed at low temperature, and the hydrodynamic damping rate for a collisional system would scale as ω^2/γ. Hence, the observed behavior of the damping rate and hydrodynamic frequency signal superfluid hydrodynamics.[23,32]

4. TOOLS FOR THERMODYNAMIC MEASUREMENTS

Equilibrium thermodynamic properties of the trapped gas, as well as dynamical properties, can be measured as functions of the temperature or of the total energy. The temperature is changed by adding energy to the gas at fixed total atom number and fixed magnetic field, starting from the lowest temperature samples. In the following, we describe first a method for precisely adding a known energy to the gas. Then we describe a method for associating an empirical temperature with the spatial profile of the gas, and a temperature calibration method using theoretically predicted spatial profiles.[58]

4.1. Precision Energy Input

Energy is added to the gas by abruptly releasing the cloud and then recapturing it after a short expansion time t_{heat}. During the expansion time, the total kinetic and interaction energy is conserved. When the trapping potential $U(\mathbf{x})$ is reinstated, the potential energy of the expanded gas is larger than that of the initially trapped gas, increasing the total energy. After waiting for the cloud to reach equilibrium, the sample is ready for subsequent measurements.

After recapture, the increase in the total energy, ΔE, is given by

$$\Delta E = \int d^3\mathbf{x}\,[n(\mathbf{x}, t_{heat}) - n_0(\mathbf{x})]\; U(\mathbf{x}), \tag{8}$$

where n_0 is the initial spatial distribution, and n is the spatial distribution after expansion during the time t_{heat}.

For a harmonically trapped cloud which is initially at nearly zero temperature, the total energy is close to that of the ground state, which is 3/4 of the Fermi energy per particle, i.e., $E_0 = (3/4)k_B T_F \sqrt{1+\beta}$. The energy after expansion and recapture is given by

$$E = E_0 \left[\frac{2}{3} + \frac{b_x^2(t_{heat}) + b_y^2(t_{heat})}{6}\right]. \tag{9}$$

Eq. 9 has a simple physical interpretation. After release from a harmonic trap, and subsequent recapture after a time t_{heat}, the potential energy in each transverse direction is increased as the square of the expansion factors, b_x and b_y, where $b_z(t_{heat}) \simeq 1$, for the conditions of our experiments. The total potential energy is half of the total energy, since the unitary gas obeys the virial theorem for an ideal gas at all temperatures, as shown in § 4.2. Hence, the initial potential energy in each direction is 1/6 of the total energy. Note that using Eq. 8, the corrections to the energy change arising from trap anharmonicity are readily determined.[31]

4.2. Test of the Virial Theorem

To test the virial theorem prediction, the gas is evaporatively cooled to the lowest temperature and then the energy is increased as described above. For each value of t_{heat}, E is calculated according to Eq. 9. For each final energy, the gas is released and the transverse radius of the cloud is measured after a *fixed* expansion time of 1 ms. The observed linear scaling of $\langle x^2 \rangle$ with the calculated E, Fig. 2 verifies the virial theorem prediction.

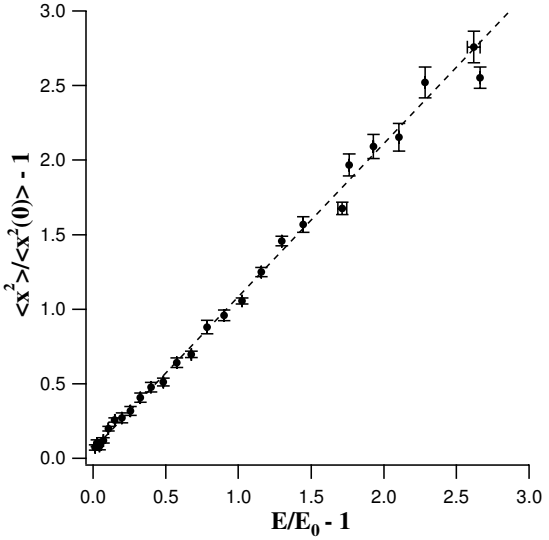

Figure 2. $\langle x^2 \rangle / \langle x^2(0) \rangle$ versus E/E_0 for a unitary gas of ^{6}Li, showing linear scaling, and verifying the virial theorem prediction. Here $\langle x^2 \rangle$ is the measured transverse mean square size. E is the total energy, calculated using Eq. 9. E_0 and $\langle x^2(0) \rangle$ denote the ground state values.

4.3. Empirical Temperature Measurement

Measurement of temperature in a noninteracting or weakly interacting Fermi gas is readily accomplished by fitting a Thomas-Fermi (T-F) distribution to the spatial profile of the cloud either in the trap, or after ballistic expansion, which alters the profile by a scale factor.[5,57] We normally integrate the measured column density of the expanded cloud over the axial dimension, and obtain the spatial profile in one transverse dimension, $n_{TF}[x; \sigma_x, T/T_F]$. The spatial profile is taken to be a function of two parameters, the Fermi radius σ_x, i.e., the cloud radius at zero temperature, and the reduced temperature T/T_F, i.e., the ratio of the Boltzmann temperature T to the trap Fermi temperature for a noninteracting gas, T_F.

One can consider $\sigma_x = \sqrt{2k_B T_F/(m\omega_x^2)}$ to set the length scale of the spatial profile and T/T_F as a shape parameter. At low T/T_F, the shape approaches a zero temperature T-F profile, $\propto (1 - x^2/\sigma_x^2)^{5/2}$, while at high T/T_F, the profile approaches a Maxwell-Boltzmann shape $\propto \exp[-m\omega_x^2 x^2/(2k_B T)] = \exp[-(x^2/\sigma_x^2)(T_F/T)]$.

In the latter case, only the product of T/T_F and σ_x^2 appears. Hence, for determination of the reduced temperature, it is convenient to determine the Fermi radius from the lowest temperature data, and then to hold this radius constant, i.e., to take $\sigma_x = c_x N^{1/6}$ in subsequent measurements at higher temperature, where c_x is held constant. In this way, the reduced temperature T/T_F is uniquely correlated with (and can be used to parametrize) the shape of the spatial profile.

For a unitary gas, the spatial profile is not precisely known in general, and there are no simple analytical formulae except at $T = 0$, as discussed above. Although the spatial profile of a unitary gas is not precisely known, we observe experimentally that the binned, one-dimensional shape is closely approximated by a T-F profile for a noninteracting gas. Further, recent theoretical predictions of the spatial profile[58] show that the one-dimensional shape is nearly of the T-F form at all temperatures, as a consequence of the existence of preformed pairs. Hence, to provide a parametrization of the spatial profiles, we take the one dimensional spatial profile of the cloud to be

of the form $n_{TF}(x;\sigma'_x,\tilde{T})$, and thereby define an *empirical* reduced temperature $\tilde{T} \equiv (T/T_F)_{fit}$ which is obtained from the fit.

In general, the empirical reduced temperature does not directly determine the reduced temperature T/T_F. However, at $T = 0$, the T-F shape is exact, so that $\tilde{T} = 0$ coincides with $T/T_F = 0$. Hence, the procedure for determining σ'_x from the data at very low temperature, where $\tilde{T} \simeq 0$, is consistent, i.e., we take $\sigma'_x = c'_x N^{1/6}$, where c'_x is held constant after obtaining it from the lowest temperature data.

Further, at sufficiently high temperature, the cloud profile must have a Maxwell-Boltzmann form $\propto \exp[-m\omega_x^2 x^2/(2k_B T)] = \exp[-(x^2/\sigma_x'^2)(1/\tilde{T})]$. This determines the natural reduced temperature scale, $\tilde{T}_{nat}$,

$$\tilde{T}_{nat} = \frac{T}{T_F\sqrt{1+\beta}}, \tag{10}$$

which follows from the interacting gas Fermi radius, $\sigma'_x = \sigma_x\,(1+\beta)^{1/4}$, and the definition of the noninteracting gas Fermi radius σ_x.

The natural reduced temperature scale is therefore exact at $T = 0$ and at high temperature, for a fixed interacting gas Fermi radius (which determines β). To calibrate $\tilde{T}$ more generally, we fit profiles of the form $n_{TF}(x;\sigma'_x,\tilde{T})$ to the spatial profiles predicted as a function of T/T_F using the formalism of pseudogap theory.[31,58] The value of σ'_x is determined from the lowest temperature theoretical profile, and $\tilde{T}$ is determined for all of the predicted profiles.

If the natural temperature were the correct scale at all T, then one would expect $T/T_F = \tilde{T}\sqrt{1+\beta} = 0.71\,\tilde{T}$. Remarkably, above the predicted superfluid transition temperature, where $T_c/T_F = 0.29$, i.e., for $\tilde{T} \geq 0.45$, the natural temperature scale is in close agreement with predictions,[31] even though noncondensed pairs are believed to exist up to at least $T/T_F \simeq 0.6$, and are present in the predicted profiles. However, below the transition, for $0 < T \leq 0.29$, i.e., for $0 \leq \tilde{T} \leq 0.45$, we find that there is a systematic deviation: Here, $T/T_F = 0.54\,\tilde{T}^{2/3}$, and the natural temperature scale underestimates the reduced temperature.[31] This is reasonable, since the energy of the unitary gas, and hence the mean square cloud size, increases as a higher power of T/T_F than quadratic. The full empirical temperature calibration is shown in the inset in Fig. 4.

5. HEAT CAPACITY

The techniques of precision energy input and empirical temperature measurement provide a method for exploring the heat capacity[31,55] of a Fermi gas. In the experiments, the ^{6}Li gas is cooled to very low temperature. For the noninteracting gas, evaporative cooling is performed at 300 G for 15 seconds. The cloud is measured at 528 G, where the scattering length is zero, and the gas is noninteracting. Energy is added as described above, except that the gas expands ballistically. Then T/T_F is measured by fitting the cloud profile with a T-F shape. Fig. 3 shows the data. The lowest temperature obtained is $T/T_F = 0.24$. For that point, E is determined from the ratio of the measured mean square cloud size according to Eq. 3, and $E_0 = 3k_B T_F/4$ is estimated from the trap frequencies and the measured number of atoms. For all other points, the energy is calculated according to Eq. 9 using ballistic scale factors.

For the unitary gas, rapid evaporative cooling for a few seconds yields $\tilde{T} \simeq 0.04$ at 840 G, just above the center of the Feshbach resonance. Then, the gas is heated by adding a known energy. Finally, the gas is released from the trap and allowed to expand for 1 ms. As observed above, the gas expands hydrodynamically by a scale factor, so that the shape of the expanded cloud closely approximates that of the trapped cloud, enabling a determination of $\tilde{T}$.

Using the temperature calibration, and replotting the raw data, we obtain the results shown in Fig. 4, which is given on a log scale. We find that a transition occurs at $T/T_F = 0.27$, in very good agreement with the predictions for the superfluid transition in a trapped, strongly-interacting Fermi gas, $T_c/T_F = 0.29$,[31] $T_c/T_F = 0.31$,[59] and $T_c/T_F = 0.30$.[60] We also find that the behavior of the energy with temperature is in very good agreement with the predictions.[31]

We fit a power law in T/T_F to the data above and below the transition temperature, yielding analytic approximations to the energy $E(T/T_F)$, from which the heat capacity is calculated using $C = (\partial E/\partial T)_{N,U}$,

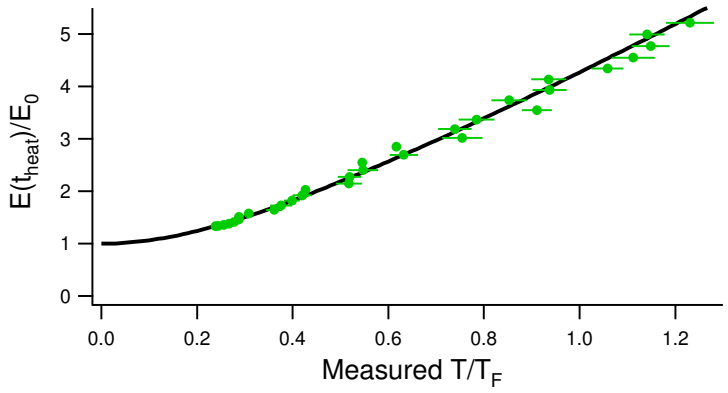

Figure 3. Total energy versus temperature for a noninteracting gas. For each heating time t_{heat}, the reduced temperature T/T_F is measured from the cloud profile, and the total energy $E(t_{heat})$ is calculated from Eq. (9) in units of the ground state energy $E_0 = 3k_BT_F/4$. Circles: noninteracting Fermi gas data. Solid curve: predicted energy versus reduced temperature for a noninteracting, trapped Fermi gas, $E_{ideal}(T/T_F)/E_{ideal}(0)$.

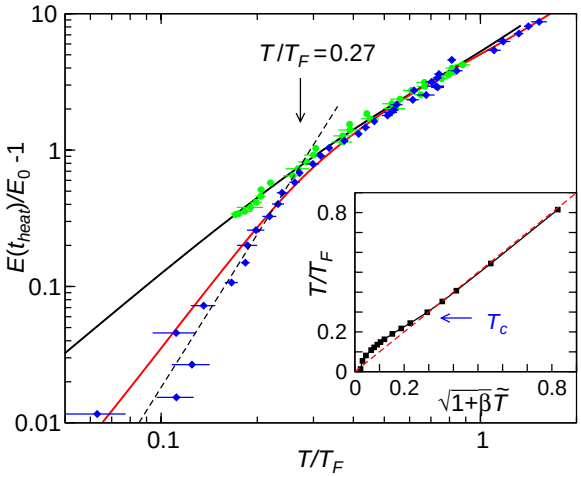

Figure 4. Energy input versus temperature, after temperature calibration, on a $log-log$ scale. The strongly-interacting Fermi gas shows a transition in behavior near $T/T_F = 0.27$. Circles: noninteracting Fermi gas data; Diamonds: strongly-interacting Fermi gas data; Lower (upper) solid curves: prediction for a unitary (noninteracting), trapped Fermi gas, calculated at trap depth $U_0/E_F = 14.6$ as in the experiments; Dashed line: best fit power law $97.3\,(T/T_F)^{3.73}$ to the calibrated unitary data for $T/T_F \leq 0.27$. The inset shows the calibration curve, which has been applied to the unitary data (diamonds). The diagonal dashed line in the inset represents $T/T_F = \sqrt{1+\beta}\,\tilde{T}$. Here $E_0 \equiv E(T=0)$, and $E_F = k_BT_F$ is the noninteracting gas Fermi energy.

where the number N and trap depth U are constant in the experiments. For $T/T_F \leq 0.27$, we obtain $E/E_0 - 1 = 97.3\,(T/T_F)^{3.73}$, while for $T/T_F \geq 0.27$, $E/E_0 - 1 = 4.98\,(T/T_F)^{1.43}$. By differentiating the energy in each region with respect to T, we find that the heat capacity exhibits a jump at the transition temperature, comparable in size to that expected for a transition between a BCS superfluid and a normal fluid.[31]

The appearance of a transition in the behavior in the heat capacity, i.e., in the behavior of the energy versus temperature, is model-independent, as it appears in the empirical temperature data, $E(\tilde{T})/E_0$, without calibration.[55] However, the estimate of the transition temperature T_c/T_F and the magnitude of the jump in heat capacity are model-dependent, since the temperature estimates are obtained by calibration using the theoretical spatial profiles.

6. SOUND VELOCITY IN BOSE AND FERMI SUPERFLUIDS

Measurement of the sound propagation from the deep molecular BEC regime to the Fermi superfluid regime allows quantitative tests of modern crossover theories. In contrast to the heat capacity experiments, during the evaporation for the sound propagation experiments, the trap U_0 is reduced by a factor of 1000. Then the field is slowly tuned to the value of interest between 710 and 1000 G. For most experiments on the Bose side of the resonance, after tuning B, the forced evaporation is continued further to trap depths as low as $\simeq 1/2000$ of the initial value. Most of the experiments with molecular BECs are done at that lowest trap depth to minimize molecular decay and subsequent heating. No thermal component is observed in the molecular BEC clouds used for the sound propagation experiment. The thermal wings appear if the cooling efficiency is reduced significantly. For experiments at the resonant magnetic field and above, on the Fermi side, the gas preparation is finished by raising the trap to a higher depth (reducing trap anharmonicity effects), after which the gas thermalizes for 0.1 s. For the low trap depth measurements, neither the measured sound speed nor the trap oscillation frequencies are corrected for anharmonicity.

The sound excitation method is similar to the one used for a BEC of atoms.[61] A thin slice of green light traverses the trapped cloud near one end. The green light at 532 nm is blue detuned from the 671 nm transition in ^{6}Li, creating a knife which locally repels the atoms. The 1/e width of the knife is $\simeq 30$ μm, and the height of the potential is chosen between 1 and 4 μK, depending on the trap depth. This beam is pulsed on for 280 μs, by cutting the beam with a magnetically actuated pinhole at the focus of a telescope, and produces two dips propagating in the opposite directions along the cloud. We let the perturbation propagate for a variable amount of time and then release the cloud, let it expand for a fixed time, and image destructively. Propagation of the density perturbation is shown in Figure 5.

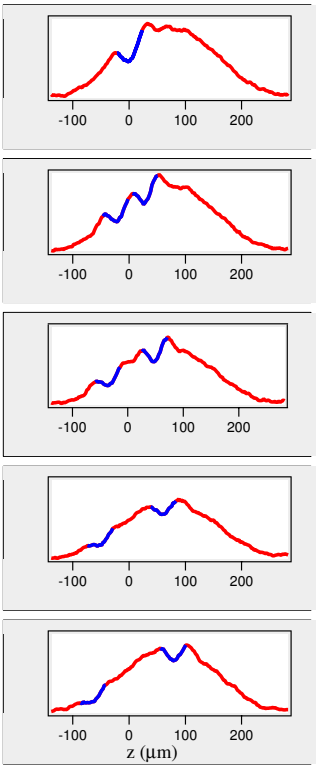

Figure 5. Sound propagation: Integrated axial profiles of the cloud for different in-trap propagation times of 0, 1, 2, 3 and 4 ms (top to bottom). Note forward and backward propagating dips.

Positions of propagating features versus the in-trap propagation time are shown in Fig. 6. Dots starting at $z = 0$ represent the coordinates of the two dips travelling in opposite directions. The upper dots are the positions

of the bulge travelling in front of the right-going dip. For the speed of sound we take the slope of the line fitting coordinates of the right-going dip.

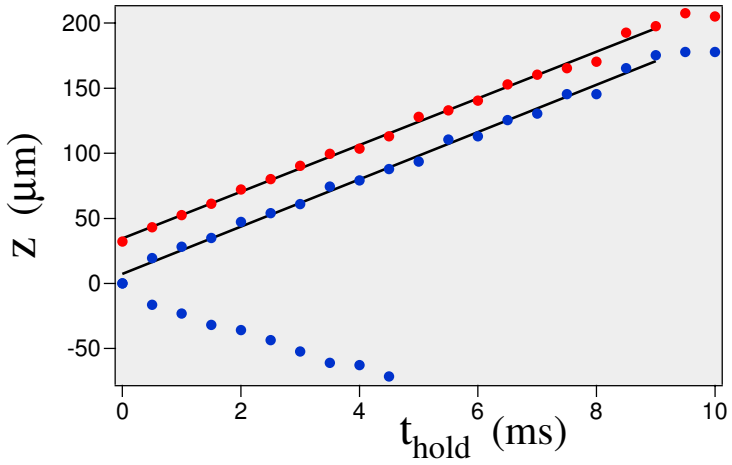

Figure 6. Axial positions of the propagating features vs time. Dots are position versus time for left- and right-propagating dips (origin at $z = 0$) as well as the right-going bulge (topmost line with dots).

The magnetic field was varied from 710 G (weakly-interacting molecular BEC regime) to 1000 G (Fermi weak pairing regime). In Figure 7, the speed of sound is plotted versus the dimensionless parameter $1/(k_F a)$, as defined above. At $T = 0$ this is the only parameter determining the physics of the system. Sound speeds are given in units of the Fermi velocity for a noninteracting gas, $v_F = \sqrt{2k_B T_F/m}$.

We observe sound propagation at all $1/(k_F a) > -1$. On the far Fermi side of the Feshbach resonance, at $1/(k_F a) < -1$, the hole created by the blue-detuned beam pulse simply fills, and the sound wave does not propagate, in contrast to the predictions which assume superfluid hydrodynamic behavior at all $1/(k_F a)$. In this region of weak pairing, sound propagation is likely to be suppressed by breaking of atomic Cooper pairs, as suggested for collective mode experiments.[24,25] Alternatively, the excitation may be too weak to observe.

Extension of the sound data deep into the molecular BEC regime lets us test the data against a simple Thomas–Fermi mean-field theory. We assume that at $1/(k_F a) > 1$, all atoms are associated into molecular dimers, and that the molecular scattering length is $a_{mol} = 0.6\, a$.[64,65] By averaging over the Thomas–Fermi density distribution of harmonically trapped BEC,[66] we obtain the average speed of sound $\bar{c}$,

$$\bar{c}/v_F = 0.28\,(k_F a)^{1/5}, \tag{11}$$

which is shown as the asymptote in Fig. 7 by a dotted line. In the molecular BEC regime, this result is in good agreement with the measurements, confirming the predicted molecular scattering length in the near resonance regime. By contrast, using the naive result $a_{mol} = 2\, a(B)$, we obtain a much larger sound speed than measured, and poor agreement.

The sound velocity c at resonance is readily estimated by using arguments based on universal thermodynamics which yield the pressure at zero temperature.[40,54] Averaging the sound speed over the density of the trapped gas, we obtain,

$$\bar{c}/v_F = 0.45\,(1+\beta)^{1/4}. \tag{12}$$

Measurement of the sound speed therefore provides a new measurement of the universal interaction parameter β.

We find that the sound speed at resonance scales as the trap depth $U^{0.26}$, very close to that expected for a harmonic trap, where $c \propto v_F \propto U^{0.25}$. Using Eq. 12, we find $\beta = -0.60 \pm 0.03$ @ 834 G. The errors denote the statistical variation obtained by averaging over all trap depths from 0.5% to 5% of full trap depth. This result

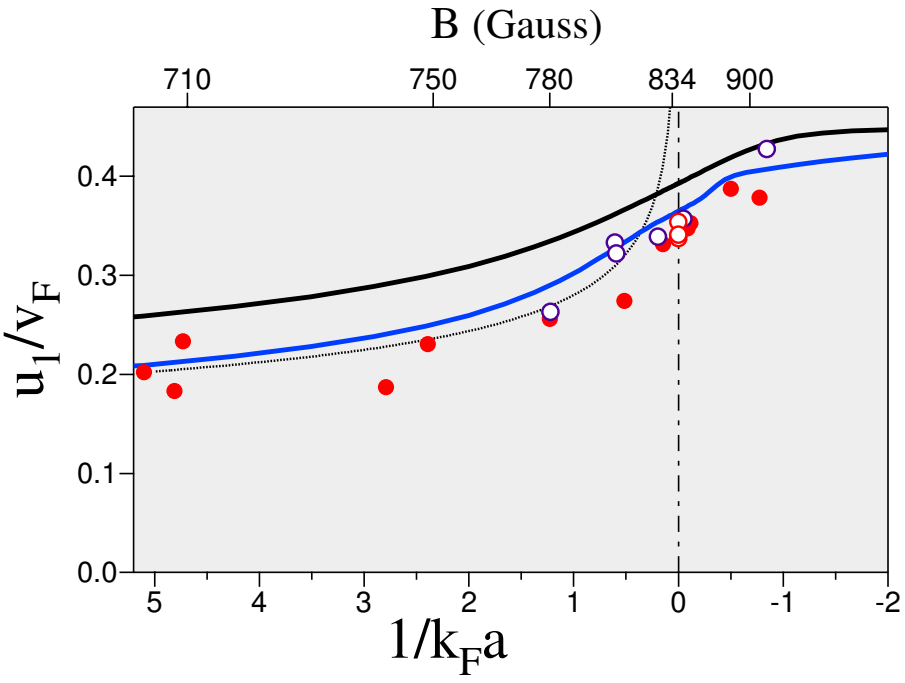

Figure 7. Speed of sound in the BEC–BCS crossover vs the interaction parameter, $1/(k_F a)$. The corresponding magnetic field B is shown on the top axis. Dots represent data taken at different trap depth U_0: open circles, $U_0 = 12$ μK; and solid dots, $U_0 = 200 - 440$ nK. Upper solid curve – mean-field theory using Leggett ground state.[62] Lower solid curve – quantum Monte Carlo calculation.[63] Dotted black line – simple Thomas–Fermi theory for the molecular BEC, using $a_{mol} = 0.6\, a$.

is somewhat larger in magnitude than the value $\beta = -0.51 \pm 0.04$ which we have obtained from the cloud size as described above.

In Fig. 7 the upper black curve represents the theory based on using the Leggett ground state[62] in all regimes. The lower solid curve is based on the equation of state obtained from quantum Monte Carlo calculations.[49,63] We can see that the Leggett state theory does not reproduce the data in the unitary and BEC regime. The Monte Carlo calculation agrees with the data quite well.

7. CONCLUSIONS

Optical traps are ideally suited for producing and manipulating ultracold quantum gases. Using all-optical techniques, we have studied a highly-degenerate, strongly-interacting Fermi gas, which is prepared by direct evaporation at a Feshbach resonance in an optical trap. By precisely adding energy to the gas, we have verified that the virial theorem holds, despite strong interactions, demonstrating universal behavior. We also observe universal behavior in the collective mode frequency, and find evidence for superfluid hydrodynamics. Sound velocity measurements enable new tests of the equation of state of the gas.

7.1. Acknowledgments

This research is supported by the Army Research Office and the National Science Foundation, the Physics for Exploration program of the National Aeronautics and Space Administration, and the Chemical Sciences, Geosciences and Biosciences Division of the Office of Basic Energy Sciences, Office of Science, U. S. Department of Energy.

REFERENCES

1. M. D. Barrett, J. A. Sauer, and M. S. Chapman, "All-optical formation of an atomic Bose-Einstein condensate," *Phys. Rev. Lett* **87**, p. 010404, 2001.
2. R. Dumke, M. Johanning, E. Gomez, J. D. Weinstein, K. M. Jones, and P. D. Lett, "All-optical generation and photoassociative probing of sodium Bose-Einstein condensates," *New J. Phys.* **8**, p. 64, 2006.
3. S. Jochim, M. Bartenstein, A. Altmeyer, G. Hendl, S. Riedl, C. Chin, J. H. Denschlag, and R. Grimm, "Bose-Einstein condensation of molecules," *Science* **302**, p. 2101, 2003.
4. S. R. Granade, M. E. Gehm, K. M. O'Hara, and J. E. Thomas, "All-optical production of a degenerate Fermi gas," *Phys. Rev. Lett.* **88**, p. 120405, 2002.
5. K. M. O'Hara, S. L. Hemmer, M. E. Gehm, S. R. Granade, and J. E. Thomas, "Observation of a strongly interacting degenerate Fermi gas of atoms," *Science* **298**, p. 2179, 2002.
6. S. Jochim, M. Bartenstein, A. Altmeyer, G. Hendl, C. Chin, J. H. Denschlag, and R. Grimm, "Pure gas of optically trapped molecules created from fermionic atoms," *Phys. Rev. Lett.* **91**, p. 240402, 2003.
7. J. D. Miller, R. A. Cline, and D. J. Heinzen, "Far-off-resonance optical trapping of atoms," *Phys. Rev. A* **47**, p. R4567, 1993.
8. T. Takekoshi and R. Knize, "CO_2 laser trap for cesium atoms," *Opt. Lett.* **21**, p. 77, 1996.
9. T. A. Savard, K. M. O'Hara, and J. E. Thomas, "Laser-noise-induced heating in far-off resonance optical traps," *Phys. Rev. A* **56**, p. 1095(R), 1997.
10. M. E. Gehm, K. M. O'Hara, T. A. Savard, and J. E. Thomas, "Dynamics of noise-induced heating in atom traps," *Phys. Rev. A* **58**, p. 3914, 1999.
11. S. Bali, K. M. O'Hara, M. E. Gehm, S. R. Granade, and J. E. Thomas, "Quantum-diffractive background gas collisions in atom-trap heating and loss," *Phys. Rev. A* **60**, p. R29, 1999.
12. H. C. W. Beijerinck, "Heating rates in collisionally opaque alkali-metal atom traps: Role of secondary collisions," *Phys. Rev. A* **62**, p. 063614, 2000.
13. K. M. O'Hara, M. E. Gehm, S. R. Granade, and J. E. Thomas, "Scaling laws for evaporative cooling in time-dependent optical traps," *Phys. Rev. A* **64**, p. 051403(R), 2001.
14. J. Stenger, S. Inouye, M. R. Andrews, H.-J. Miesner, D. M. Stamper-Kurn, and W. Ketterle, "Strongly enhanced inelastic collisions in a Bose-Einstein condensate near Feshbach resonances," *Phys. Rev. Lett* **82**, p. 2422, 1999.
15. J. E. Thomas and M. E. Gehm, "Optically trapped Fermi gases," *Am. Scientist* **92**, p. 238, 2004.
16. H. Heiselberg, "Fermi systems with long scattering lengths," *Phys. Rev. A* **63**, p. 043606, 2001.
17. G. A. Baker, Jr., "Neutron matter model," *Phys. Rev. C* **60**, p. 054311, 1999.
18. J. Carlson, S.-Y. Chang, V. R. Pandharipande, and K. E. Schmidt, "Superfluid Fermi gases with large scattering length," *Phys. Rev. Lett.* **91**, p. 050401, 2003.
19. P. F. Kolb and U. Heinz, *Quark Gluon Plasma 3*, p. 634. World Scientific, 2003.
20. Q. J. Chen, J. Stajic, S. N. Tan, and K. Levin, "BCS-BEC crossover: From high temperature superconductors to ultracold superfluids," *Phys. Rep.* **412**, pp. 1–88, 2005.
21. M. Houbiers, R. Ferwerda, H. T. C. Stoof, W. I. McAlexander, C. A. Sackett, and R. G. Hulet, "Superfluid state of atomic ^{6}Li in a magnetic trap," *Phys. Rev. A* **56**, p. 4864, Dec 1997.
22. M. Houbiers, H. T. C. Stoof, W. I. McAlexander, and R. G. Hulet, "Elastic and inelastic collisions of ^{6}Li atoms in magnetic and optical traps," *Phys. Rev. A* **57**(3), p. R1497, 1998.
23. J. Kinast, S. L. Hemmer, M. E. Gehm, A. Turlapov, and J. E. Thomas, "Evidence for superfluidity in a resonantly interacting Fermi gas," *Phys. Rev. Lett.* **92**, p. 150402, 2004.
24. M. Bartenstein, A. Altmeyer, S. Riedl, S. Jochim, C. Chin, J. H. Denschlag, and R. Grimm, "Collective excitations of a degenerate Fermi gas at the BEC-BCS crossover," *Phys. Rev. Lett.* **92**, p. 203201, 2004.
25. J. Kinast, A. Turlapov, and J. E. Thomas, "Breakdown of hydrodynamics in the radial breathing mode of a strongly-interacting Fermi gas," *Phys. Rev. A* **70**, p. 051401(R), 2004.
26. C. A. Regal, M. Greiner, and D. S. Jin, "Observation of resonance condensation of fermionic atom pairs," *Phys. Rev. Lett.* **92**, p. 040403, 2004.

27. M. W. Zwierlein, C. A. Stan, C. H. Schunck, S. M. F. Raupach, A. J. Kerman, and W. Ketterle, "Condensation of fermionic atom pairs near a Feshbach resonance," *Phys. Rev. Lett.* **92**, p. 120403, 2004.
28. C. Chin, M. Bartenstein, A. Altmeyer, S. Riedl, S. Jochim, J. H. Denschlag, and R. Grimm, "Observation of the pairing gap in a strongly interacting Fermi gas," *Science* **305**, p. 1128, 2004.
29. M. Greiner, C. A. Regal, and D. S. Jin, "Probing the excitation spectrum of a Fermi gas in the BCS-BEC crossover regime," *Phys. Rev. Lett.* **94**, p. 070403, 2005.
30. G. B. Partridge, K. E. Strecker, R. I. Kamar, M. W. Jack, and R. G. Hulet, "Molecular probe of pairing in the BEC-BCS crossover," *Phys. Rev. Lett.* **95**, p. 020404, 2005.
31. J. Kinast, A. Turlapov, J. E. Thomas, Q. Chen, J. Stajic, and K. Levin, "Heat capacity of strongly-interacting Fermi gas," *Science* **307**, p. 1296, 2005.
32. J. Kinast, A. Turlapov, and J. E. Thomas, "Damping in a unitary Fermi gas," *Phys. Rev. Lett.* **94**, p. 170404, 2005.
33. M. Zwierlein, J. Abo-Shaeer, A. Schirotzek, C. Schunck, and W. Ketterle, "Vortices and superfluidity in a strongly interacting Fermi gas," *Nature* **435**, p. 1047, 2005.
34. C. A. R. S. de Melo, M. Randeria, and J. R. Engelbrecht, "Crossover from BCS to Bose superconductivity: Transition temperature and time-dependent Ginzburg-Landau theory," *Phys. Rev. Lett.* **71**, p. 3202, 1993.
35. J. V. Steele, "Effective field theory power counting at finite density." nucl-th/0010066, 2000.
36. M. Greiner, C. A. Regal, and D. S. Jin, "Emergence of a molecular Bose-Einstein condensate from a Fermi gas," *Nature* **426**, p. 537, 2003.
37. M. W. Zwierlein, C. A. Stan, C. H. Schunck, S. M. F. Raupach, S. Gupta, Z. Hadzibabic, and W. Ketterle, "Observation of Bose-Einstein condensation of molecules," *Phys. Rev. Lett.* **91**, p. 250401, 2003.
38. T. Bourdel, L. Khaykovich, J. Cubizolles, J. Zhang, F. Chevy, M. Teichmann, L. Tarruell, S. Kokkelmans, and C. Salomon, "Experimental study of the BEC-BCS crossover region in lithium 6," *Phys. Rev. Lett.* **93**, p. 050401, 2004.
39. M. E. Gehm, S. L. Hemmer, S. R. Granade, K. M. O'Hara, and J. E. Thomas, "Mechanical stability of a strongly interacting Fermi gas of atoms," *Phys. Rev. A* **68**, p. 011401(R), 2003.
40. T.-L. Ho, "Universal thermodynamics of degenerate quantum gases in the unitarity limit," *Phys. Rev. Lett.* **92**, p. 090402, 2004.
41. A. Perali, P. Pieri, and G. C. Strinati, "Quantitative comparison between theoretical predictions and experimental results for the BCS-BEC crossover," *Phys. Rev. Lett.* **93**(10), p. 100404, 2004.
42. N. Manini and L. Salasnich, "Bulk and collective properties of a dilute Fermi gas in the BCS-BEC crossover," *Phys. Rev. A* **71**, p. 033625, 2005.
43. D. Lee, "Ground state energy of spin-1/2 fermions in the unitary limit," *Phys. Rev. B* **73**, p. 115112, 2006.
44. A. Bulgac, J. E. Drut, and P. Magierski, "Spin 1/2 fermions in the unitary regime: A superfluid of a new type," *Phys. Rev. Lett.* **96**, p. 090404, 2006.
45. M. Bartenstein, A. Altmeyer, S. Riedl, S. Jochim, C. Chin, J. H. Denschlag, and R. Grimm, "Crossover from a molecular Bose-Einstein condensate to a degenerate Fermi gas," *Phys. Rev. Lett.* **92**, p. 120401, 2004.
46. G. B. Partridge, W. Li, R. I. Kamar, Y. Liao, and R. G. Hulet, "Pairing and phase separation in a polarized Fermi gas," *Science* **311**, p. 503, 2006.
47. T. Bourdel, J. Cubizolles, L. Khaykovich, K. M. F. Magãlhaes, S. Kokkelmans, G. V. Shlyapnikov, and C. Salomon, "Measurement of the interaction energy near a Feshbach resonance in a ^{6}Li Fermi gas," *Phys. Rev. Lett.* **91**, p. 020402, 2003.
48. C. A. Regal, M. Greiner, S. Giorgini, M. Holland, and D. S. Jin, "Momentum distribution of a Fermi gas of atoms in the BCS-BEC crossover," *Phys. Rev. Lett.* **95**, p. 250404, 2005.
49. T. K. Ghosh and K. Machida, "Sound velocity and multibranch bogoiubov spectrum of an elongated Fermi superfluid in the BCS-BEC crossover," *Phys. Rev. A* **73**, p. 013613, 2005.
50. H. Heiselberg, "Sound modes at the BCS-BEC crossover," *Phys. Rev. A* **73**, p. 013607, 2006.
51. P. Capuzzi, P. Vignolo, F. Federici, and M. P. Tosi, "Sound propagation in elongated superfluid fermionic clouds," *Phys. Rev. A* **73**, p. 021603(R), 2006.
52. G. E. Astrakharchik, J. Boronat, J. Casulleras, and S. Giorgini, "Equation of state of a Fermi gas in the BEC-BCS crossover: A quantum Monte Carlo study," *Phys. Rev. Lett.* **93**, p. 200404, 2004.

53. M. Bartenstein, A. Altmeyer, S. Riedl, R. Geursen, S. Jochim, C. Chin, J. H. Denschlag, R. Grimm, A. Simoni, E. Tiesinga, C. J. Williams, and P. S. Julienne, "Precise determination of ^{6}Li cold collision parameters by radio-frequency spectroscopy on weakly bound molecules," *Phys. Rev. Lett.* **94**, p. 103201, 2005.
54. J. E. Thomas, A. Turlapov, and J. Kinast, "Virial theorem and universality in a unitary Fermi gas," *Phys. Rev. Lett.* **95**, p. 120402, 2005.
55. J. Kinast, A. Turlapov, and J. E. Thomas, "Heat capacity of a strongly-interacting Fermi gas." arXiv:cond-mat/0409283, 2004.
56. C. Chin, "Simple mean-field model for condensates in the BEC-BCS crossover regime," *Phys. Rev. A* **72**, p. 041601(R), 2005.
57. C. Menotti, P. Pedri, and S. Stringari, "Expansion of an interacting Fermi gas," *Phys. Rev. Lett.* **89**, p. 250402, 2002.
58. J. Stajic, Q. Chen, and K. Levin, "Density profiles of strongly interacting trapped Fermi gases," *Phys. Rev. Lett.* **94**, p. 060401, 2005.
59. A. Perali, P. Pieri, L. Pisani, and G. C. Strinati, "BCS-BEC crossover at finite temperature for superfluid trapped Fermi atoms," *Phys. Rev. Lett.* **92**(22), p. 220404, 2004.
60. P. Massignan, G. M. Bruun, and H. Smith, "Viscous relaxation and collective oscillations in a trapped Fermi gas near the unitarity limit," *Phys. Rev. A* **71**, p. 033607, 2005.
61. M. R. Andrews, D. M. Kurn, H.-J. Miesner, D. S. Durfee, C. G. Townsend, S. Inouye, and W. Ketterle, "Propagation of sound in a Bose-Einstein condensate," *Phys. Rev. Lett.* **79**, p. 554, 1997.
62. K. Levin Private communication., 2006.
63. G. Astrakharchik Private communication., 2006.
64. D. S. Petrov, C. Salomon, and G. V. Shlyapnikov, "Weakly bound dimers of fermionic atoms," *Phys. Rev. Lett* **93**, p. 090404, 2004.
65. G. E. Astrakharchik, J. Boronat, J. Casulleras, and S. Giorgini, "Equation of state of a Fermi gas in the BEC-BCS crossover: A quantum Monte-Carlo study," *Phys. Rev. Lett* **93**, p. 200404, 2004.
66. F. Dalfovo, S. Giorgini, L. P. Pitaevski, and S. Stringari, "Theory of Bose-Einstein condensation in trapped gases," *Rev. Mod. Phys.* **71**, pp. 463–512, 1999.